Quantification of Biomechanical Interaction of Transcatheter Aortic Valve Stent Deployed in Porcine and Ovine Hearts

Joseph Mummert, Eric Sirois, and Wei Sun

Tissue Mechanics Lab, Biomedical Engineering Program and Mechanical Engineering Department, University of Connecticut, 207 Bronwell Building, Storrs, CT 06269-3139, USA

Associate Editor Jane Grande-Allen oversaw the review of this article.

Abstract—Success of the deployment and function in transcatheter aortic valve replacement is heavily reliant on the tissue–stent interaction. The present study quantified important tissue–stent contact variables of self-expanding transcatheter aortic valve stents when deployed into ovine and porcine aortic roots, such as the stent radial expansion force, stent pullout force, the annulus deformation response and the coefficient of friction on the tissue–stent contact interface. Braided Nitinol stents were developed, tested to determine stent crimped diameter vs. stent radial force from a stent crimp experiment, and deployed *in vitro* to quantify stent pullout, aortic annulus deformation, and the coefficient of friction between the stent and the aortic tissue from an aortic root–stent interaction experiment. The results indicated that when crimped at body temperature from 26 mm to 19, 21 and 23 mm stent radial forces were approximately 30–40% higher than those crimped at room temperature. Coefficients of friction leveled to approximately 0.10 ± 0.01 as stent wire diameter increased and annulus size decreased from 23 to 19 mm. Regardless of aortic annulus size and species tested, it appeared that a minimum of about 2.5 mm in annular dilatation, caused by about 60 N of radial force from stent expansion, was needed to anchor the stent against a pullout into the left ventricle. The study of the contact biomechanics in animal aortic tissues may help us better understand characteristics of tissue–stent interactions and quantify the baseline responses of non-calcified aortic tissues.

Keywords—Transcatheter aortic valves, Self-expanding, Radial force, Biomechanics.

INTRODUCTION

Since the first procedure in 2002,[5] there has been an explosive growth in transcatheter aortic valve replacement (TAVR). By the end of 2011, there were 10 transcatheter aortic valve (TAV) companies that had first-in-man implantation data. Four of these 10 TAV devices have received the CE Mark and are used clinically in Europe.[22] About 50,000 TAVRs have been performed worldwide. Short- and medium-term outcomes after TAVR is encouraging with significant reduction in rates of death. However, adverse events associated with TAVR have been detected, including stroke, myocardial infarction, peripheral embolism, injury to the aorta, perivalvular leak, and access site injury.[11,32] Furthermore, long-term durability and safety of these valves are largely unknown and need to be evaluated and studied carefully.[17,31,33] Successful deployment and function in TAVR is heavily reliant on the tissue–stent interaction. For instance, excessive radial force of the stent may cause aortic injury, while insufficient force may lead to paravalvular leakage and device migration. Therefore, a better understanding of the aortic tissue–TAV interaction is critical to TAVR success.

Important stent–tissue interactive parameters include the stent radial expansion force, the associated aortic annulus deformation, the stent axial pullout force and the coefficient of friction at the contact interface. Engineering analyses to quantify the values of these parameters, using either computational methods or *in vitro* experiments, have been limited. Computational methods have been utilized to simulate the biomechanical interaction between the aortic root and TAV stent.[3,8,23,26,27,30] Dwyer *et al.*[8] used computational fluid dynamics (CFD) simulations to quantify forces that could potentially dislodge the prosthesis. They reported that the peak dislodge force during diastole was 6.01 N, approximately an order of magnitude greater than the peak force during systole (0.60 N). Sun *et al.*[26] conducted finite element analysis

Address correspondence to Wei Sun, Tissue Mechanics Lab, Biomedical Engineering Program and Mechanical Engineering Department, University of Connecticut, 207 Bronwell Building, Storrs, CT 06269-3139, USA. Electronic mail: weisun@engr.uconn.edu

(FEA) of TAV deformation and reported axial force values in the range of 5.8–6.1 N after applying a static diastolic pressure to the TAV leaflets. Tzamtzis *et al.*[27] conducted numeric analyses of the radial expansion forces of size 26 mm Medtronic CoreValve and Edwards Sapien TAVs. The CoreValve exerted hoop forces in the 2–7 N range when deployed in 20–23 mm of the aortic annulus and the Sapien hoop force was about 12–14 N, varying dependent on the stiffness of size 22 mm aortic annulus. These computational studies offered scientific insight into the stent–tissue interaction; however, they were limited by the lack of experimental tissue data to validate the simulation results.

Animal models have been considered as an effective measure of assessing valve performance prior to use in humans. In recent years, more than 40 journal articles have been published on animal trials of various transcatheter valve interventions, with about 500 porcine, ovine, and bovine animals used.[2,4,6,10,13,14,18–20,29,36] A review by Gallegos *et al.*[9] reported that ovine (78%) and porcine (9.5%) models were the most commonly used in valve research. Even though the validity of porcine and ovine models in TAV implantation trials is a subject of debate,[15,16] quantification of interactive responses of stent deployment into an animal root can provide baseline values for evaluating stent performance and the aortic root deformation, before studying more complicated scenarios with aged and calcified human roots.

In this study, we developed a self-expanding woven TAV stent. The woven stent was braided from Nitinol wire, thus its radial expansion force can be varied when braided with wire of different diameters. We quantified the stent crimp diameter vs. stent radial force relationship using a stent crimp experiment. Then, the stent was deployed *in vitro* in porcine and ovine hearts. The stent radial expansion force, pullout force and coefficient of friction at the stent–tissue contact interface were quantified. Lastly, we assessed TAV migration potential and highlighted the selection of TAV based upon the amount of oversizing needed to support physiologic loads.

MATERIALS AND METHODS

Stent Crimp Experiment

Nitinol wires with wire diameters of 0.014″, 0.016″, 0.017″, 0.022″ were obtained from Memry Corporation, Bethel, CT, USA (meets ASTM F2063-05). Self-expanding Nitinol stents were fabricated using these four types of wires. No valve leaflet was incorporated into the TAV stent as shown in Fig. 1a. The stent geometry was a straight tube with a height of 16 mm

and a diameter of 26 mm. The stent was composed of four strut cells in the axial and twelve in the circumferential directions. A heat treatment of 8 min at 500 °C was utilized to set the stent geometry. The stents were labeled as type 1–4 according to the wire diameters of 0.014″, 0.016″, 0.017″, 0.022″, respectively.

A stent crimp experiment was performed to quantify the radial expansion force of the Nitinol stents. Briefly, as illustrated in Fig. 1b, the experiment setup consisted of a Dacron strap that was wrapped around the stent, and mounted on a Tinius Olsen uniaxial testing apparatus (Model H50K-S, Horsham, PA, USA). One end was clamped and fastened between two stainless steel plates containing a narrow slit such that the Dacron strap could be pulled evenly and clamped at the opposing end. A Dacron strap was chosen because of its rigidity, which exhibited insignificant strain under the loading of this experiment. The stent diameter was determined from fixture displacement and verified by the images taken on the stent central area. Hoop force from the strap (Fig. 1c) was measured by a load cell attached on the uniaxial machine. The experiments were conducted at room temperature and at 37 °C in order to quantify the temperature effect on the stent radial expansion force.

To convert the hoop force, measured from the load cell, to the radial expansion force of the stent, we utilized the force equilibrium established in the horizontal direction as shown in Fig. 1c, such that the hoop force can be determinated in terms of contact pressure (P), stent radius (r), and stent contact length (L),

$$2 \cdot F_{\text{hoop}} = P \cdot 2 \cdot r \cdot L. \tag{1}$$

The radial expansion force (F_{Radial}), or the total contact force, can be defined as,

$$F_{\text{Radial}} = P \cdot A_{\text{Interior–Contact}} = P \cdot 2 \cdot \pi \cdot r \cdot L. \tag{2}$$

Thus, we have

$$F_{\text{Radial}} = 2 \cdot \pi \cdot F_{\text{hoop}}. \tag{3}$$

Aortic Root–Stent Interaction Experiment

Porcine hearts ($n = 12$, 6–9 months old) and ovine hearts ($n = 12$, 1–2 year old) from Animal Technologies, Inc. (Tyler, TX, USA) were obtained fresh and stored in a −80 °C freezer for a maximum of 3 weeks before testing. Prior to testing, each frozen heart was held at room temperature (20 °C) for 30 min and then placed in a 37 °C water bath until defrosted.[1] The hearts were weighed and the aortic annulus size was measured with aortic sizers (Edwards Lifesciences LLC). For the porcine hearts, 3 of them had an
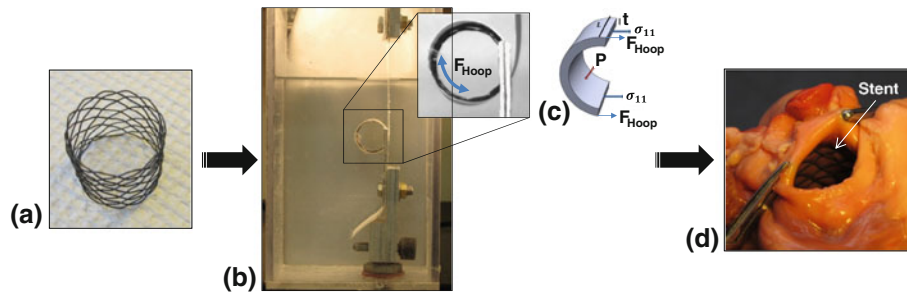
FIGURE 1. (a) Stent design. (b) Stent crimp experimental setup to measure hoop force at body temperature (37 °C). (c) Free body diagram of stent cross-section labeled to show hoop force exerted on transcatheter valve stent from Dacron strap. (d) Stent *in situ*.

annulus size of 19 mm, 7 had an annulus size of 21 mm and 2 had a size of 23 mm. For the ovine hearts, 4 hearts had each of annulus sizes of 19, 21 and 23 mm. The entire heart was then submerged in a clear-sided tank (21 mm long × 18 mm wide × 18 mm high and 2.8 mm thick) filled with a Ca^{2+}-free and glucose-free Tyrode solution[21] to minimize active contraction of the muscle fibers. The solution of the tank was maintained at either room temperature or body temperature of 37 °C.

Tissue specimens were subjected to preconditioning by inflating a percutaneous transluminal valvuloplasty balloon (Z-Med II-X, NuMED, Inc., Denton, TX, USA) to a diameter 1 mm larger than the initially sized diameter for a total of ten cycles. Each of the 4 TAV stents were sequentially implanted—4 stents per heart in order of increasing wire diameter—into the aortic root with the middle of the TAV stent height aligned with the aortic annulus (Fig. 1e). The targeted deployment was directed such that half of the device was above and below the aortic annulus. After the TAV stent was deployed, the stent was post-dilated by the valvuloplasty balloon and the final diameter of the stent was used to deduce the radial force based on the experimental data obtained in section "Stent Crimp Experiment". The purpose of a post-deployment dilatation of the stent was to ensure that the stent was under the same loading state as it was in the crimped diameter vs. radial force relationship of section "Stent Crimp Experiment". It should be noted that a Nitinol material has different stress vs. strain responses in loading and unloading states as shown in Fig. 2.[7]

An ultrasound probe (75L60EA Ultrasonic Transducer, Mindray Bio-Medical Electronics Co.) was placed on the front end of the tank to capture two-dimensional cross-sectional images of the TAV stent deployed inside the aortic root at the tissue–stent contact equilibrium position. Ultrasound images were collected at the top, middle, and bottom of the stent. All images were analyzed by identifying regions of different image intensity. Image intensities are distinguishable between tissue, water and the stent. The stent
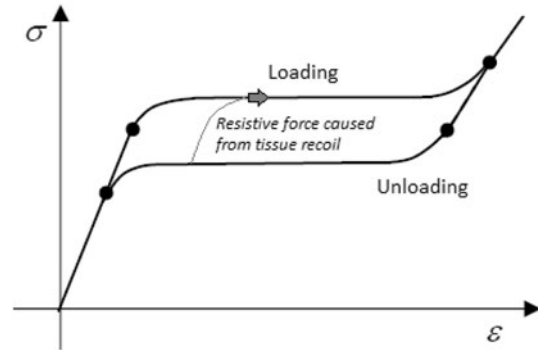

FIGURE 2. A typical stress–strain curve illustrating the path dependence of Nitinol during deployment into the aortic annulus.

diameter was measured by selecting pixel values along the outer rim of the stent.

From the tissue biomechanics perspective, it is important to know how much radial force is needed to expand the aortic root to a certain size. By deploying the four stents into the aortic root, four data points of the expanded aortic annulus diameter vs. the radial force, derived from the crimped stent diameter, were obtained. As a result, these four stents essentially served as a measurement gauge to quantify biomechanical responses of the aortic root when subjected to a radial expansion force.

The TAV stent was then pulled out of the intact valve and the pullout force was recorded. Briefly, in this experiment, the apex of the heart was dissected off and the heart was reverse oriented (apex of the heart facing up) in the same fluid filled tank. Stiff polymer strings which had previously been attached around the circumference of the bottom of the TAV stent were attached to the uniaxial testing apparatus. The polymer strings were then pulled in the direction of the apex at a constant speed of 20 mm/min. At the aortic root–TAV stent interface, the coefficient of friction (μ) was calculated from the radial force and pullout force values. By applying Amontons-Coulomb friction law,[28] the pullout force $F_{Pullout}$ may be defined by

$$F_{\text{Pullout}} = \mu F_{\text{Radial}}. \tag{4}$$

Each heart was tested with the four types of TAV stents and the pullout force experiment was repeated four times per TAV stent.

During diastole, the closed TAV leaflets are subjected to an *in vivo* axial pullout force that may contribute to valve migration. We approximated this *in vivo* pullout force, $F_{\text{Pullout-in vivo}}$ on the TAV stent by estimating the transvalvular pressure and the projected stent cross-sectional area along the axial direction of the stent:

$$F_{\text{Pullout}-in\ vivo} = \Delta P_{\text{stent}} \cdot A_{\text{projected}} = \Delta P_{\text{stent}} \pi \left(\frac{d}{2}\right)^2_{\text{stent}}. \tag{5}$$

A TAV stent with an experimental pullout force F_{Pullout} less than the calculated diastolic pressure pullout force $F_{\text{Pullout}-in\ vivo}$ may migrate into the left ventricle at physiological transvalvular pressure.

RESULTS

Experimental Results

Illustrated in Fig. 3a are the representative curves of the stent diameter vs. radial force for the four types of stents tested at body and room temperatures. It can be seen that the radial force increased with a larger stent wire diameter, as one would expect. As the stent diameter was crimped down from 24 to 17 mm, an average of 1.5–2.0 times of increase of the radial force was required. When the diameters were crimped to smaller than 17 mm or from 26 to 24 mm, the required force increased much more rapidly. The stent responses when they were crimped from 26 mm to 19, 21 and 23 mm were examined in detail. It can be seen in Fig. 3b that for each of the four types of stents, when crimped at body temperature, the stent radial forces were about 30–40% higher than those crimped at room temperature.

The aortic annulus ellipticities averaged for all animals at the stent–contact equilibrium positions were within the represented ratio range of 1:1.03 from Fig. 4.

For both porcine and ovine animal models, pullout forces were in the range of 1.8–5.3 N, 3.8–7.5 N, 5.0–8.8 N, 6.5–14.2 N for TAV stent-1, 2, 3 and 4, respectively. The pullout forces increased with larger wire diameter (Fig. 5).

By deploying a size 26 mm stent into the aortic root of an annulus size of 19, 21 and 23 mm, the effect of stent oversizing was also investigated (Fig. 5). It can be seen that the pullout force was dependent on both the amount of oversizing and the stent type. Stent-4 had a low chance of stent migration because the experimental pullout force was larger than the diastolic pressure pullout force for all three sizes of the aortic annulus, while stent-1 had a high potential of stent migration for all three sizes of the aortic annulus (Fig. 5).

Experimentally determined coefficients of friction between the native valve and TAV stent leveled to approximately 0.10 ± 0.01 as stent wire diameter increased and annulus size decreased from 23 to 19 mm (Table 1). The smallest coefficient of friction (0.05 ± 0.01) was determined when stent-1 was placed in a 23 mm aortic annulus. For TAV stent-4, the coefficient of friction had reached a stable value independent of aortic annulus size as well as animal species.

The aortic root tissue response, obtained from the aortic root–stent expansion test of twelve porcine (a–c) and twelve ovine (d–f) hearts arranged with respect to annulus size, are illustrated in Fig. 6. Note that data for the 23 mm porcine annulus size is only represented in two cases. In general, the aortic root was expanded with nonlinear responses, becoming less extensible with increasing dilatation. Porcine samples exhibited similar dilatation and radial force ranges to ovine samples. Inter-specimen differences were also small.

A clear distinction was observed for tissue responses with different animal annulus diameters. A much higher stent radial force was required to dilate an annulus of diameter 19 mm to a diameter greater than 23.4 mm (an equivalent tissue strain of 23%), when compared to a similar dilatation in an annulus diameter of 21 mm (Figs. 6c, 6f). As the tissues were dilated to an annulus diameter greater than 3.5–4 mm, a more pronounced upslope curve was observed, indicating increased tissue stiffening. On the contrary, in an annulus size of 23 mm, the circumferential strain range was only of the low toe region and no upslope in the curve was present (Figs. 6a, 6d). Thus, the extracted radial interactive force was dependent on the structural response of the aortic root; progressive stiffening occurred with increased annular dilatation.

TAV Stent–Tissue Pairings

The estimated diastolic pressure forces were between 4.2–6.0 N, 4.9–6.3 N, and 5.8–6.7 N for an aortic annulus of size 19, 21, and 23 mm, respectively (Table 2). Vertical arrows on Fig. 6 highlight the location of the dilated annulus diameter where the calculated peak diastolic pressure pullout force was located on the fitted experimental pullout force curve. The horizontal arrows then point to the radial force needed to resist a pullout. Regardless of aortic annulus size, it appeared that a minimum of about 2.5 mm in
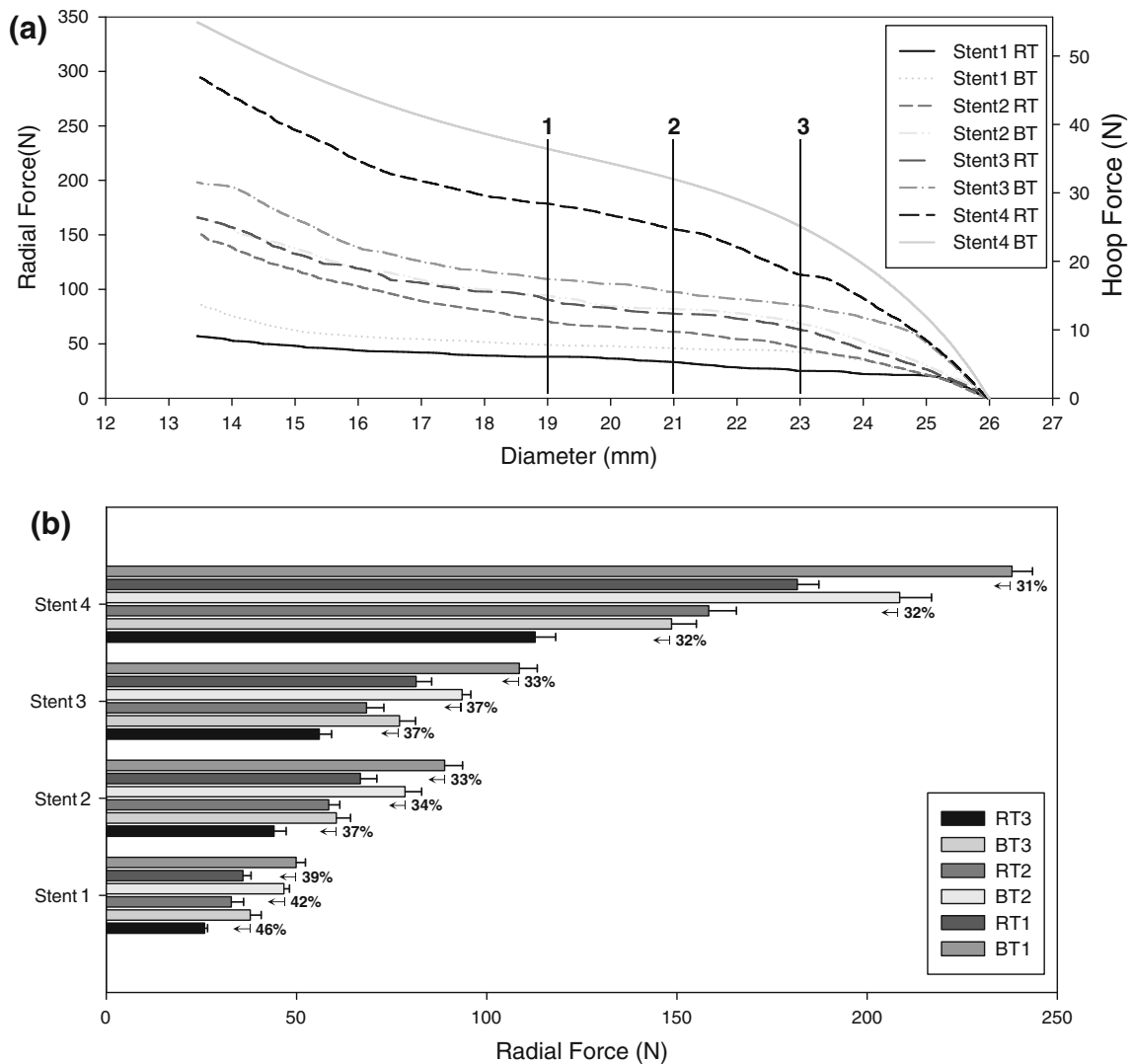
FIGURE 3.   (a) Representative stent crimp diameter vs. radial force relationship of the four stents tested at (b) $n = 4$, crimped from 26 mm to 19, 21, and 23 mm, respectively (RT = room temperature; BT = body temperature).

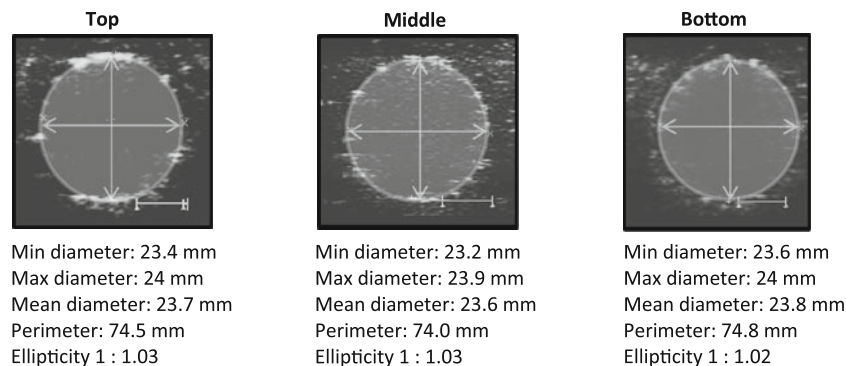| Top	Middle	Bottom
Min diameter: 23.4 mm	Min diameter: 23.2 mm	Min diameter: 23.6 mm
Max diameter: 24 mm	Max diameter: 23.9 mm	Max diameter: 24 mm
Mean diameter: 23.7 mm	Mean diameter: 23.6 mm	Mean diameter: 23.8 mm
Perimeter: 74.5 mm	Perimeter: 74.0 mm	Perimeter: 74.8 mm
Ellipticity 1 : 1.03	Ellipticity 1 : 1.03	Ellipticity 1 : 1.02

FIGURE 4.   Ultrasound measurement of the tissue–stent contact equilibrium positions from a sized 21 mm aortic annulus. Minimal inter-specimen differences in aortic annulus ellipticity at the contact equilibrium positions *ex vivo* were observed.

annular dilatation, caused by about 60 N of radial force from stent expansion, was needed to anchor the stent. A 2.5 mm tissue dilatation equated to an 11–13% circumferential strain at the annulus, i.e., 11% strain in 23 mm aortic annulus to 13% strain in 19 mm aortic annulus.
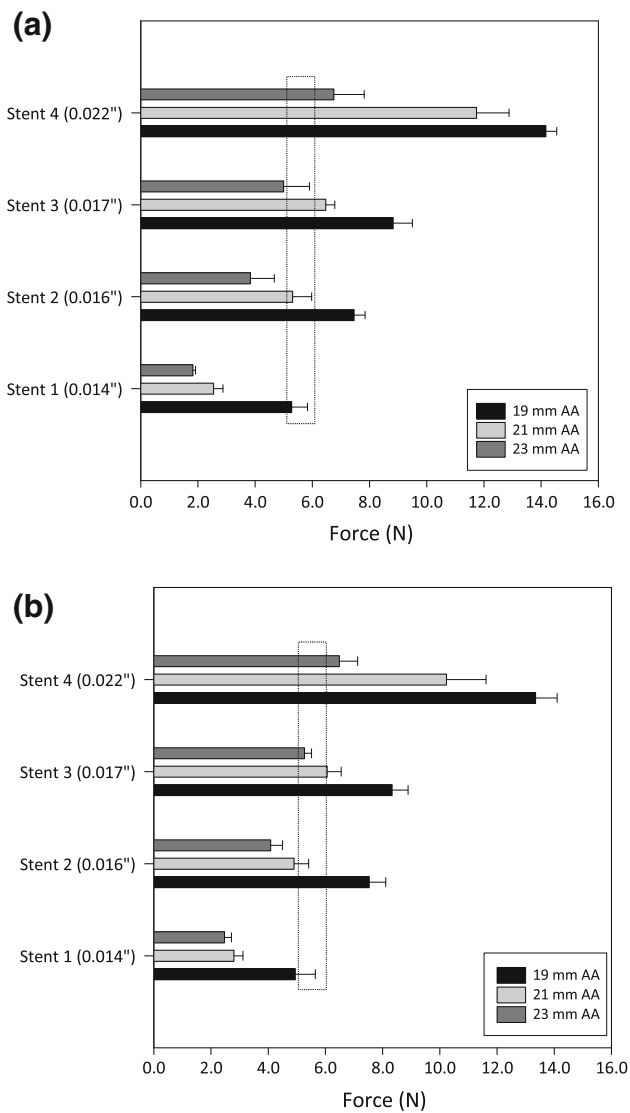
(a)

(b)

FIGURE 5. Pullout force vs. stent, listed for the three native aortic annulus (AA) sizes and grouped into porcine (a) and ovine (b). Dotted box indicates the estimated *in vivo* pullout force for an annulus diameter of size 21 mm, as calculated in section ''Aortic Root–Stent Interaction Experiment'' and reported in Table 2.

DISCUSSION

Success of the deployment and function in TAVR depends largely upon the contact interaction between the tissue and device. Adverse events such as paravalvular leakage, device migration, and aortic dissection may be minimized with accurate valve sizing. The current practice is to measure the patient's aortic annulus size and select a stent that is oversized. However, there is a lack of rigorous engineering analysis of tissue–stent contact variables such as stent radial force, pullout force, aortic annulus deformation, and the coefficient of friction between the stent and the aortic tissue. The present study described an experimental study to measure expansion forces of self-expanding TAV stents and investigated tissue behaviors after the stents were deployed into the ovine and porcine hearts.

Nitinol Stent Crimp Response

Our braided TAV stents had similar relationships of the crimped diameter vs. expansion force compared to those of other TAV stents reported in the literature. Zegdi *et al.*[35] developed braided self-expandable Nitinol stents (Laboratoires Perouse, France) and tested radial force using a loop strap method similar to our study. In the study, two 26 mm stents, one stiffer than the other, were deployed into 88 patients intraoperatively and retrieved after 2 min. At a crimped diameter of 19 mm, their softer stent reported a hoop force of 6 N, equivalent to a radial force of 38 N, whereas their stiffer stent produced a hoop force of 11 N, equivalent to 69 N of radial force.[35] As seen from our study in Fig. 3b, stent-1 acted similar to the softer stent of Zegdi *et al.* and stent-3 behaved similar to the stiffer stent in the same study. Another study by Tzamtzis *et al.*[27] reported hoop forces between 7 and 11 N, equivalent to radial forces of 44–69 N, respectively, for a 26 mm Medtronic CoreValve device at a 19 mm crimped diameter size, which were also similar to the stents examined in this study.

TABLE 1. Coefficient of friction (μ) between the aortic root and transcatheter valve stent.

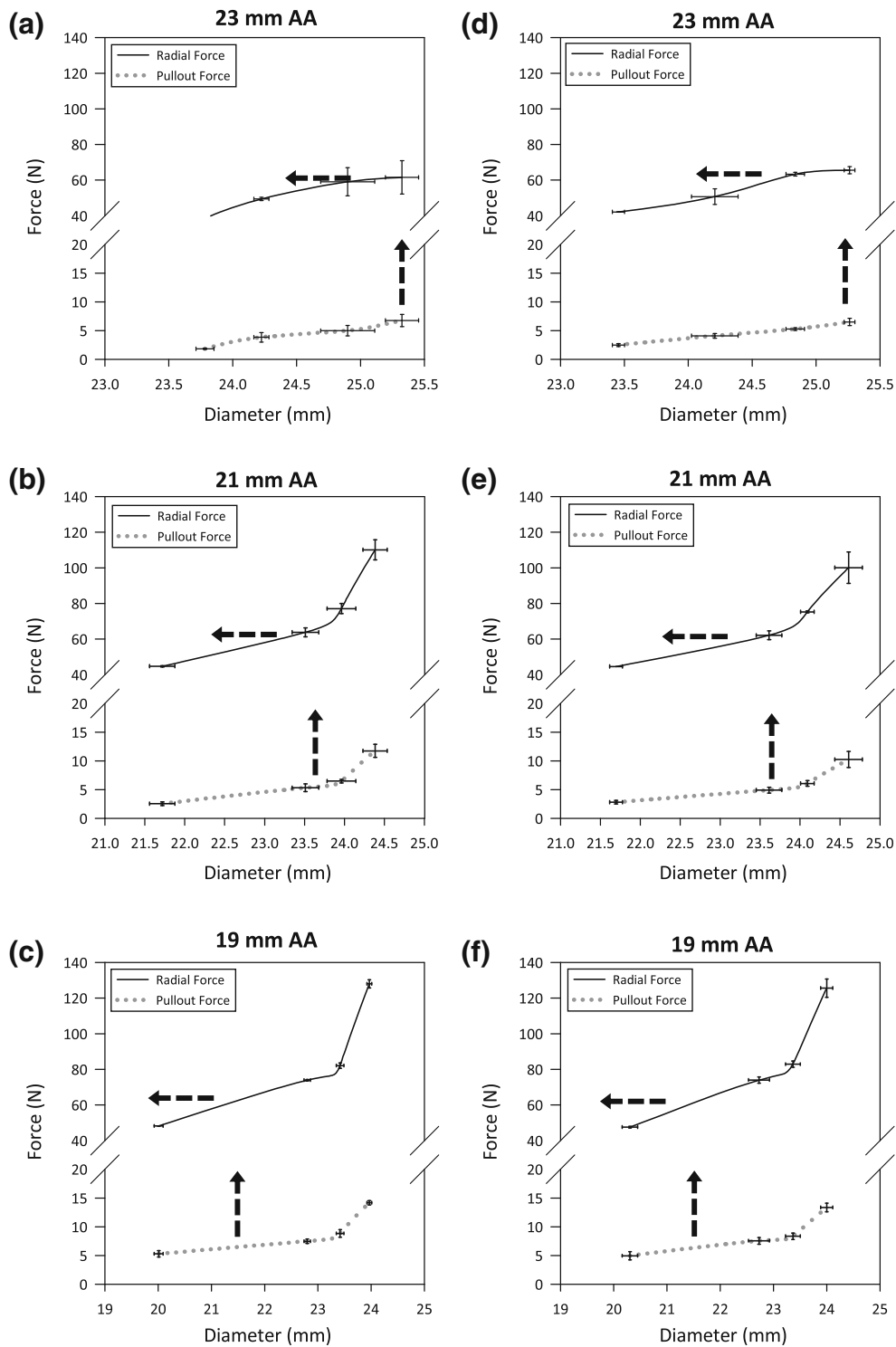|	Specimen			μ			
	Aortic annulus size (mm)	n	Mass (g)	Stent 1 (0.014'')	Stent 2 (0.016'')	Stent 3 (0.017'')	Stent 4 (0.022'')
Porcine	19	3	396 ± 40	0.10 ± 0.01	0.10 ± 0.01	0.10 ± 0.01	0.11 ± 0.01
	21	7	416 ± 58	0.06 ± 0.01	0.08 ± 0.01	0.08 ± 0.01	0.10 ± 0.01
	23	2	468 ± 80	0.05 ± 0.01	0.08 ± 0.01	0.08 ± 0.01	0.10 ± 0.01
Ovine	19	4	392 ± 71	0.10 ± 0.01	0.10 ± 0.01	0.10 ± 0.01	0.10 ± 0.01
	21	4	477 ± 44	0.06 ± 0.01	0.08 ± 0.01	0.08 ± 0.01	0.10 ± 0.01
	23	4	491 ± 23	0.06 ± 0.01	0.08 ± 0.01	0.08 ± 0.01	0.10 ± 0.01

FIGURE 6. Biomechanical tissue behavior of the aortic root tested in (a–c) porcine and (d–f) ovine tissue grouped according to aortic annulus (AA) diameter sizes 19, 21, and 23 mm. Vertical arrows are provided to show the location of the dilated annulus diameter where the calculated peak diastolic pressure pullout force, as reported in Table 2, occurred on the experimental pullout force curve. Horizontal arrows are provided to show the radial force extracted at this annulus diameter position.

Since Nitinol material exhibits different loading–unloading behavior (Fig. 2), in this study, we performed a post-deployment dilation of the TAV stents such that the stents were under a loading state, instead of an unloading state, to match with the stent crimp experiment setup. Post-deployment dilation of the

TABLE 2. Axial diastolic pressure pullout forces on transcatheter valve stent.

Aortic annulus size (mm)	$D_{eq\text{-}min}$ (mm)	$D_{eq\text{-}max}$ (mm)	$\Delta P_{TAV\ stent}$ (mmHg)	Force$_{min}$ (N)	Force$_{max}$ (N)
19	20	24	100	4.2	6.0
21	21.7	24.6	100	4.9	6.3
23	23.5	25.3	100	5.8	6.7

D_{eq} = equilibrium position after a 26 mm diameter TAV stent was deployed inside the aortic root. $\Delta P_{TAV\ stent}$ = approximation of the pressure gradient across the TAV stent.

Medtronic CoreValve may also be performed at the discretion of the interventional cardiologist depending on initial assessment of the deployment.[34] In addition, TAV Nitinol stents exhibit temperature-dependent stiffness, as shown in Fig. 3. Previous studies indicate that by controlling the A_f temperature during processing, the apparent stiffness of the stent will change. For each degree that the transition temperature is below body temperature, the loading and unloading forces increase by nearly 4 N/mm^2.[7,25] This thermal response is represented in our data even though we were not given an exact A_f value. While A_f control was not manipulated or investigated in this study, it is important to mention because a lower A_f will produce a stiffer stent.

Animal Tissue Response

Trivial annulus-dependent differences between porcine and ovine aortic tissue may indicate that both animal types are equivalent models for pre-clinical biomechanical evaluation of TAV stents. As the radial interactive force increased upon contact, tissue stiffness increased nonlinearly, which is typical of aortic tissue.[12] This profile was best seen when the TAV stents were deployed in an annulus diameter of size 19 mm.

Stiffness of the aortic annulus may be estimated using the data in Fig. 6. Note that this estimation does not incorporate annulus wall thickness because of the inhomogeneity in the annulus region. Based on the Law of Laplace, the annulus wall tension T can be obtained from, $T = pr$. Utilizing Eq. (2), T may be expressed as $T = \frac{F_{radial}}{2\pi L}$. Herein, we chose one data point from Fig. 6, as an example, to illustrate our estimation of the stiffness of the aortic annulus. We use the data from stent-2 when it was deployed into a porcine annulus of 21 mm. From Fig. 6, it can be seen that the dilated annulus diameter was 23.5 mm and the radial expansion force was about 63 N. If we assume the stent contact length L is about 10 mm, then the annulus wall tension is about 1 MPa. The annulus strain ε is about 0.12. Thus, the stiffness of the aortic

annulus is estimated to be about 8.33 MPa. To appreciate this stiffness value, we compared it with biaxial mechanical testing data of porcine ascending aorta.[15] At a similar strain of 0.12, the stiffness of porcine ascending aortic tissue is about 0.41 MPa, suggesting the annulus is a region of much higher stiffness. It is questionable whether the myocardium's role is significant, but the fibrous continuity between the aortic and mitral valve is much stiffer than the aortic sinus and ascending aorta. Further studies to quantify detailed material properties of the tissues in the annulus region are warranted.

Accurate Sizing

The current industry recommendation is to oversize the TAV with respect to the diameter of the native aortic annulus, e.g., a 26 mm CoreValve is designed for 20–23 mm annulus sizes.[24] From the annulus deformation responses shown in Fig. 6, it can be seen that when the tissue–stent reach a force equilibrium that resists the pullout from the axial *in vivo* force, the minimal required annulus dilation, caused by the expansion force from the stent, is about 2.5 mm. The minimal expansion force from the stent is about 60 N. We observed this minimum of 2.5 mm dilation and 60 N of radial force consistently for all sizes of annulus tested in this study regardless of animal species.

This information is important for the stent design in that if a 26 mm stent is deployed into the non-calcified annulus sizes of 20–23 mm, the minimal diameter of annulus after the deployment might be around 22.5–25.5 mm, at which the valve should open and close properly. In another words, the valve might be designed to operate in the functional diameter of 22.5–25.5 mm. A stent designed with a stronger radial stiffness, such as using a larger stent wire diameter, would then allow for a smaller stent oversizing.

In addition, we showed that to counter retrograde migration forces, a minimum of 60 N interactive radial force might be required to anchor a TAV stent. Figure 7 illustrated possible TAV stent-patient annulus matching, such that a selected stent would support physiologic forces and exert a radial force to resist stent migration. As an example, for the 26 mm TAV stents fabricated in this study, TAV stent-2 and -3 are shown to offer adequate force, achieving an annular dilation criterion of 2.5 mm and can be implanted safely in 19 and 21 mm aortic annuluses, respectively. TAV stent-2, oversized by 7 mm in a 19 mm annulus, appeared to rest at a tissue–stent equilibrium diameter of 22.7 ± 0.01 mm. TAV stent-3, oversized by 5 mm in a 21 mm annulus, appeared to rest at a tissue–stent equilibrium diameter of 24.1 ± 0.01 mm. Note that TAV stent-1, regardless of oversize amount, did not

FIGURE 7. Transcatheter valve stent–tissue pairings. Oversize measure and corresponding equilibrium diameter position (D_{eq}) for TAV stents offering an expansion force that meets the minimal required annulus dilation to counter migration in non-calcified aortic tissue.

exert enough radial force to achieve an annular dilation of 2.5 mm, thus, will likely fail during implantation.

Quantifying radial interactive forces of various stents allowed for appropriate TAV stent selection of a particular oversize as indicated in Fig. 7. Provided with these baseline responses, it should be noted that patients with calcification can have a smaller degree of valve oversizing.

Limitations

A static analysis was conducted, i.e., the aortic root dynamic motion as well as tissue growth and remodeling in a long-term application were not considered. Determination of the radial interactive force using *in vitro* experiments implies that the tissue responses induced by the stent were based on passive material properties. Because the TAV stents were sequentially implanted, there may be potential tissue weakening introduced from the forced removal of an earlier implant. Due to limited availability, human tissue was not used in this study. Calcification was not incorporated into our model. Calcium deposition will increase the tissue stiffness and the coefficient of friction. A higher coefficient of friction due to calcification might help anchor the stent. A future direction is to use a calcified human aortic root model. Finally, two-dimensional planar imaging was used to determine the tissue–stent equilibrium position. Three-dimensional echocardiography, or computed tomography, could enhance the accuracy of aortic annulus assessment. It must be recognized that the data presented here cannot be directly applied to human conditions. The animal models may not be representative of human conditions. The stents used in the study are not directly comparable to current approved devices used to treat aortic stenosis.

CONCLUSIONS

The progression and success in TAVR is reliant on the understanding of the biomechanics involved at the device-aortic wall interface. In this study, we investigated important parameters that govern aortic root–TAV interaction: stent radial and pullout forces, tissue responses upon the deployment of the TAV stent, and coefficient of friction at the stent–tissue interface. While patients who receive this treatment typically have calcified valves, the study of the interacting contact mechanics at the non-calcified level may help us understand characteristics of tissue–stent interactions and quantify the baseline responses of non-calcified aortic tissues.

REFERENCES

[1]Bia, D., *et al.* Cryopreservation procedure does not modify human carotid homografts mechanical properties: an isobaric and dynamic analysis. *Cell Tissue Banking* 7:183–194, 2006.

[2]Boudjemline, Y., *et al.* Steps toward the percutaneous replacement of atrioventricular valves: an experimental study. *J. Am. Coll. Cardiol.* 46(2):360–365, 2005.

[3]Capelli, C., *et al.* Patient-specific simulations of transcatheter aortic valve stent implantation. *Med. Biol. Eng. Comput.* 50(2):183–192, 2012.

[4]Cribier, A., H. Eltchaninoff, and N. Borenstein. Transcatheter implantation of a baloon-expandable prosthetic heart valves: early results in an animal model. *Circulation* 11(Suppl. 11):11–552, 2001.

[5]Cribier, A., *et al.* Percutaneous transcatheter implantation of an aortic valve prosthesis for calcific aortic stenosis: first human case description. *Circulation* 106(24):3006–3008, 2002.

[6]Dewey, T. M., *et al.* Transapical aortic valve implantation: an animal feasibility study. *Ann. Thorac. Surg.* 82(1):110–116, 2006.

[7]Duerig, T. W., D. E. Tolomeo, and M. Wholey. An overview of superelastic stent design. *Minim. Invasive Ther. Allied Technol.* 9(3–4):235–246, 2000.

[8]Dwyer, H., *et al.* Migration forces of transcatheter aortic valves in patients with noncalcific aortic insufficiency. *J. Thorac. Cardiovasc. Surg.* 138(5):1227–1233, 2009.

[9]Gallegos, R. P., *et al.* The current state of in-vivo preclinical animal models for heart valve evaluation. *J. Heart Valve Dis.* 14(3):423–432, 2005.

[10]Garay, F., *et al.* The Cribier-Edwards percutaneous heart valve in the pulmonic position: initial animal experience. *EuroInterv. Suppl.* 1(Supplement A):A32–A35, 2006.

[11]Grube, E., *et al.* Percutaneous aortic valve replacement for severe aortic stenosis in high-risk patients using the second- and current third-generation self-expanding CoreValve prosthesis: device success and 30-day clinical outcome. *J. Am. Coll. Cardiol.* 1(50):69–76, 2007.

[12]Humphrey, J. D. Cardiovascular Solid Mechanics: Cells, Tissues, and Organs. New York: Springer, vol. xvi, 2002.

[13]Lauten, A., *et al.* Experimental evaluation of the JenaClip transcatheter aortic valve. *Catheter. Cardiovasc. Interv.* 74(3):514–519, 2009.

[14]Lutter, G., *et al.* Percutaneous aortic valve replacement: an experimental study. I. Studies on implantation. *J. Thorac. Cardiovasc. Surg.* 123(4):768–776, 2002.

[15]Martin, C., T. Pham, and W. Sun. Significant differences in the material properties between aged human and porcine aortic tissues. *Eur. J. Cardiothorac. Surg.* 40(1):28–34, 2011.

[16]Martin, C., and W. Sun. Biomechanical characterization of aortic valve tissue in humans and common animal models. *J. Biomed. Mater. Res. A* 100A(6):1591–1599, 2012.

[17]Movahed, M. Where are we going with percutaneous aortic valve replacement? *Expert Rev. Cardiovasc. Ther.* 6(5):997–998, 2007.

[18]Naqvi, T. Z., *et al.* Beating-heart percutaneous mitral valve repair using a transcatheter endovascular suturing device in an animal model. *Catheter. Cardiovasc. Interv.* 69(4):525–531, 2007.

[19]Pavcnik, D., K. C. Wright, and S. Wallace. Development and initial experimental evaluation of a prosthetic aortic valve for transcatheter placement: work in progress. *Radiology* 183(1):151–154, 1992.

[20]Pedersen, W. R., *et al.* iCoapsys mitral valve repair system: percutaneous implantation in an animal model. *Catheter. Cardiovasc. Interv.* 72(1):125–131, 2008.

[21]Pham, T., and W. Sun. Comparison of biaxial mechanical properties of coronary sinus tissues from porcine, ovine and aged human species. *J. Mech. Behav. Biomed. Mater.* 6:21–29, 2012.

[22]Rodés-Cabau, J. Transcatheter aortic valve implantation: current and future approaches. *Nat. Rev. Cardiol.* 9(1):15–29, 2012.

[23]Schoenhagen, P., *et al.* In vivo imaging and computational analysis of the aortic root. Application in clinical research and design of transcatheter aortic valve systems. *J. Cardiovasc. Transl. Res.* 4(4):459–469, 2011.

[24]Schultz, C. J., *et al.* Three dimensional evaluation of the aortic annulus using multislice computer tomography: are manufacturer's guidelines for sizing for percutaneous aortic valve replacement helpful? *Eur. Heart J.* 31(7):849–856, 2010.

[25]Stoeckel, D., A. Pelton, and T. Duerig. Self-expanding Nitinol stents: material and design considerations. *Eur. Radiol.* 14(2):292–301, 2004.

[26]Sun, W., K. Li, and E. Sirois. Simulated elliptical bioprosthetic valve deformation: implications for asymmetric transcatheter valve deployment. *J. Biomech.* 43(16):3085–3090, 2010.

[27]Tzamtzis, S., *et al.* Numerical analysis of the radial force produced by the Medtronic-CoreValve and Edwards-SAPIEN after transcatheter aortic valve implantation (TAVI). *Med. Eng. Phys.* 2012 (in press).

[28]Vad, S., *et al.* Determination of coefficient of friction for self-expanding stent-grafts. *J. Biomech. Eng.* 132(12), Article No. 121007, 2010.

[29]Walther, T., *et al.* Transapical approach for sutureless stent-fixed aortic valve implantation: experimental results. *Eur. J. Cardiothorac. Surg.* 29(5):703–708, 2006.

[30]Wang, Q., E. Sirois, and W. Sun. Patient-specific modeling of biomechanical interaction in transcatheter aortic valve deployment. *J. Biomech.* 45(11):1965–1971, 2012.

[31]Webb, J. G., and D. A. Wood. Current status of transcatheter aortic valve replacement. *J. Am. Coll. Cardiol.* 60(6):483–492, 2012.

[32]Webb, J., *et al.* Percutaneous transarterial aortic valve replacement in selected high-risk patients with aortic stenosis. *Circulation* 7(116):755–763, 2007.

[33]Ye, J., *et al.* Transapical transcatheter aortic valve implantation: follow-up to 3 years. *J. Thoracic Cardiovasc. Surg.* 139(5):1107–1113.e1, 2010.

[34]Zamorano, J. L., *et al.* EAE/ASE recommendations for the use of echocardiography in new transcatheter interventions for valvular heart disease. *Eur. Heart J.* 32(17):2189–2214, 2011.

[35]Zegdi, R., *et al.* Increased radial force improves stent deployment in tricuspid but not in bicuspid stenotic native aortic valves. *Ann. Thorac. Surg.* 89(3):768–772, 2010.

[36]Zong, G. J., *et al.* Use of a novel valve stent for transcatheter pulmonary valve replacement: an animal study. *J. Thorac. Cardiovasc. Surg.* 137(6):1363–1369, 2009.